Proteomic response analysis of a threonine-overproducing mutant of *Escherichia coli*

Yang-Hoon KIM*, Jin-Seung PARK*, Jae-Yong CHO†, Kwang Myung CHO‡, Young-Hoon PARK‡[1] and Jeewon LEE*[1]

*Department of Chemical and Biological Engineering, Korea University, Anam-Dong 5-1, Sungbuk-Ku, Seoul 136-701, South Korea, †Department of Bioindustry and Technology, Sangji University, 660 Wonju-Si, Kangwon-Do 220-702, South Korea, and ‡R&D Center for Bioproducts, Institute of Science and Technology, CJ Corporation, Ichon-Si, Kyongggi-Do 467-810, South Korea

The proteomic response of a threonine-overproducing mutant of *Escherichia coli* was quantitatively analysed by two-dimensional electrophoresis. Evidently, 12 metabolic enzymes that are involved in threonine biosynthesis showed a significant difference in intracellular protein level between the mutant and native strain. The level of malate dehydrogenase was more than 30-fold higher in the mutant strain, whereas the synthesis of citrate synthase seemed to be severely inhibited in the mutant. Therefore, in the mutant, it is probable that the conversion of oxaloacetate into citrate was severely inhibited, but the oxidation of malate to oxaloacetate was significantly up-regulated. Accumulation of oxaloacetate may direct the metabolic flow towards the biosynthetic route of aspartate, a key metabolic precursor of threonine. Synthesis of aspartase (aspartate ammonia-lyase) was significantly inhibited in the mutant strain, which might lead to the enhanced synthesis of threonine by avoiding unfavourable degradation of aspartate to fumarate and ammonia. Synthesis of threonine dehydrogenase (catalysing the degradation of threonine finally back to pyruvate) was also significantly down-regulated in the mutant. The far lower level of cystathionine β-lyase synthesis in the mutant seems to result in the accumulation of homoserine, another key precursor of threonine. In the present study, we report that the accumulation of important threonine precursors, such as oxaloacetate, aspartate and homoserine, and the inhibition of the threonine degradation pathway played a critical role in increasing the threonine biosynthesis in the *E. coli* mutant.

Key words: *Escherichia coli* mutant, proteomic response, threonine biosynthesis, two-dimensional gel electrophoresis (2-DE).

INTRODUCTION

The industrial production of amino acids using micro-organisms has expanded in terms of both the amount and number of amino acids [1–4]. Threonine is an essential amino acid necessary for the growth and maintenance of birds and mammals, and has been introduced in the agricultural industry for balancing the livestock feed [2,5]. Since the chemical synthesis does not give a high yield, industrial production of threonine has been dependent on microbial fermentation [6–8]. Previously, for increasing the yield/productivity of amino acid biosynthesis, efforts were focused more on the metabolic engineering and genetic manipulation, along with the help of increasing genome databases for diverse micro-organisms significantly [9]. Furthermore, the specific genes related to threonine biosynthesis have been cloned from various bacteria, including *Escherichia coli*, *Corynebacterium glutamicum* and *Brevibacterium* sp. [2,10–12]. Although it has long been known by molecular studies on the synthetic pathways of *E. coli* that threonine biosynthesis from aspartate requires the five-step metabolic conversion, important and novel characteristics for metabolic flux control have remained uncovered.

Several *E. coli* strains for fermentation of L-threonine were also developed through multiple rounds of mutation programmes that aimed at blocking threonine degradation pathways [6,13,14]. The results of kinetic studies of all the five key enzymes from a thiaisoleucine-resistant derivative of *E. coli* strain K12 have been reported [15], and the rational design of pathway modifications has been extensively simulated [16–18]. Despite all these efforts, strategies of mutagenesis and screening for threonine overproduction have not been established because the occurrence of undefined mutations may be accompanied in strain development [6,15,19]. For this reason, more systematic approaches have been taken through proteome analysis using 2-DE (two-dimensional gel electrophoresis) followed by MS. The 2-DE technique has been improved for comparative proteomics, requiring the reproducibility and reliability of differential protein expression analysis among samples [20–22]. Although there have been some reports on the comprehensive view of the physiological state and responses of *E. coli* metabolism in the fermentation process using proteomics tools [23,24], the proteomic approach for building a quantitative dynamic analysis and the metabolic synthetic pathway is still at an early stage of development. Nevertheless, the extended proteomics (along with the ever-increasing amount of protein sequence data and enhanced MS technology) have been proposed elsewhere as a powerful tool for the predictions and simulation of various metabolic pathways for active metabolic network [25,26].

In the present study, the proteomic responses of a threonine-overproducing mutant were studied in detail by analysing quantitatively the time-course synthesis of metabolic enzymes for threonine biosynthesis. Comparative proteome analysis showed that the threonine overproduction resulted from the significant change in the synthesis of important metabolic enzymes involved in threonine biosynthesis. Also, the correlation between degradation/accumulation of threonine (or its precursors) and the threonine overproduction has been demonstrated in detail.

Abbreviations used: ASPA, aspartate ammonia-lyase; 2-DE, two-dimensional gel electrophoresis; IPG, immobilized pH gradient; MALDI–TOF-MS, matrix-assisted laser-desorption ionization–time-of-flight mass spectrometry; METC, cystathione β-lyase; TDH, threonine dehydrogenase.

[1] Correspondence may be addressed to either author (e-mail leejw@korea.ac.kr).

EXPERIMENTAL

Bacterial strains

E. coli W3110 [F$^-$IN(*rrnD-rrnE*) *rpoS*$^-$], which produces a negligible level of threonine (< 0.1 mM), was used as a parent strain for comparative analysis [27]. The threonine-producing mutant *E. coli* (Met$^-$Ile^L AHV^r AEC^r AC^r ABA^r *rpoS*$^-$) was obtained from a previously constructed threonine-producing *E. coli* strain, TF427 [27], by mutations performed using *N*-methyl-*N*′-nitro-*N*-nitrosoguanidine. This strain requires both methionine and isoleucine for growth. *E. coli* Hfr 3000 YA73 (*thrB relA1 spoT1 thi-1*) was used for cloning of the *thr* operon [28].

Sample preparations from batch culture of *E. coli*

Strains were routinely grown in Luria–Bertani medium or M9 medium [28]. If necessary, ampicillin was used at a final concentration of 100 g/ml. *E. coli* W3110 and its threonine-producing mutant were grown in a 5-litre jar fermenter containing 1.5 litres of fermentation medium [70 g of glucose, 10 g of $(NH_4)_2SO_4$, 2 g of KH_2PO_4, 0.5 g of $MgSO_4 \cdot 7H_2O$, 5 mg of $FeSO_4 \cdot 7H_2O$, 5 mg of $MnSO_4 \cdot 4H_2O$, 3 g of yeast extract and 800 mg of methionine per litre of water at pH 6.0] [27]. A seed culture was grown at 33 °C for 4 h in a 500 ml flask containing 75 ml of modified Luria–Bertani medium and then inoculated into a 5-litre jar fermenter. During the cultivation, a mixture of glucose and phosphate at final concentrations of 60 and 0.5 g/l respectively was fed twice when the glucose level was < 5 g/l. During the batch fermentation, the pH was maintained at 6.0 with NH_4OH, the temperature was maintained at 31 °C, the aeration rate was 1 vvm (air volume · working volume^{-1} · min^{-1}), and the agitation speed was 800 rev./min. Cells were harvested at the different growth phases and adjusted to A_{600} 0.8 with 10 mM Tris buffer (pH 8.0), 100 ml of which was centrifuged at 2510 ***g*** and 4 °C for 5 min and then washed twice with 40 mM Tris buffer including 1 mM PMSF. Cell pellets were resuspended in lysis buffer [8 M urea/4 % (w/v) CHAPS/40 mM Tris/protease inhibitor cocktail solution; Roche Diagnostics GmbH, Mannheim, Germany]. After sonication for 2 min on ice, the cell debris was removed by centrifugation at 25 750 ***g*** for 60 min. The protein concentration was determined by Bio-Rad protein assay kit (Hercules, CA, U.S.A.) using BSA as a standard. The supernatants were kept at − 80 °C until used for 2-DE. Proteins (100 μg) were resuspended in rehydration solution (8 M urea/2% CHAPS/0.005 % Bromophenol Blue; final volume, 350 μl). Urea, CHAPS, Tris, dithiothreitol, Bromophenol Blue, Triton X-100 and SDS were purchased from Sigma (St. Louis, MO, U.S.A.).

2-DE and image analysis

The first step of 2-DE, isoelectric focusing, was performed on a Pharmacia Biotech IPGphor Electrophoresis System (Amersham Biosciences, Uppsala, Sweden) at 20 °C. Linear pH 4–7 IPG (immobilized pH gradient) gel strips (18 cm; Amersham Biosciences) were rehydrated overnight by placing the strips gel-side-down in sample-containing rehydration solution in the IPGphor strip holder and covering with the DryStrip Cover Fluid (Amersham Biosciences). The samples were loaded with 100 μg of intracellular protein concentrations for silver-stained gels with Seeblue plus2 marker (Invitrogen, Carlsbad, CA, U.S.A.). Isoelectric focusing was performed for 2 h at 500 V, for 0.5 h at 1000 V, for 0.5 h at 2000 V, for 0.5 h at 4000 V and finally maintained at 70 000 V · h at 8000 V in the IPGphor for analytical and preparative gels. Next, the IPG gel strips were equilibrated for 15 min in equilibration solution [50 mM Tris/HCl, pH 8.8/6 M urea/30 % (v/v) glycerol/2 % (w/v) SDS/Bromophenol Blue trace] in 1 % dithiothreitol for 15 min, and then in 2.5 % (w/v) iodoacetamide for 15 min. Equilibrated gel strips were placed on a 12.5 % polyacrylamide gel, and the second-dimensional separation was performed using a PROTEAN II Xi cell system (Bio-Rad) in a cold chamber at 4 °C. SDS/PAGE was performed at 30 mA/gel for 12 h until the Bromophenol Blue reached to the bottom of the gel. The silver stain was performed using the modified method as described in [29]. Stained gels were scanned using UMAX powerlook 1100 scanner. ImageMaster software v 4.01 (Amersham Biosciences) was used for the gel image analysis, including quantification of the spot intensities that is performed on a volume basis (i.e. values were calculated from the integration of spot optical intensity over the spot area).

MALDI–TOF-MS (matrix-assisted laser-desorption ionization–time-of-flight mass spectrometry) analysis and protein identification

Samples for the MALDI–TOF-MS analysis were extracted from silver-stained spots as described previously [30]. Enzymic digestions were performed overnight at 37 °C in stationary incubator using 10–15 μg of sequencing-grade modified trypsin/ml (Proma, WI, U.S.A.) in 25 mM ammonium bicarbonate (pH 8.0). In-gel-digested peptide fragments were extracted from gel pieces using 5 % (v/v) trifluoroacetic acid and 50 % (v/v) acetonitrile mixture, followed by vortex-mixing for 1 h. After repeatedly washing for three times, solute materials including peptide fragments were dried by vacuum centrifugation. Ziptip column (Millipore, Bedford, MA, U.S.A.) in which C_{18} resin is fixed at the end of the tip was used to eliminate impurities of samples. The peptide solution was prepared with an equal volume of saturated α-cynao-4-hydroxycinnamic acid solution in 50 % acetonitrile/0.1 % trifluoroacetic acid on a sample plate of MALDI–TOF-MS. Protein was analysed using MALDI–TOF-MS system (Voyager DE-STR, PE Biosystem, Framingham, MA, U.S.A.). Spectra were calibrated using a matrix and tryptic autodigestion ion peaks as internal standards. Peptide mass fingerprints were analysed using the MS-Fit (http://prospector.ucsf.edu/). The identification of a protein with respect to theoretical parameters (pI, molecular mass etc.) was accepted if the peptide mass matched with a mass tolerance within 10 p.p.m. The accessibility of such data has been revolutionized by the use of Internet methods such as SWISS-2D-PAGE (http://www.expasy.org/).

RESULTS AND DISCUSSION

Comparative proteome analysis: mutant versus native strain

Prior to 2-DE analysis, both wild-type and mutant strains of *E. coli* W3110 were cultivated in a batch bioreactor (5 litres). The mutant strain overproduced threonine to > 70–80 g/l in the batch culture, despite severely inhibited cell growth (results not shown). Similar growth inhibition was reported for several bacterial mutants overproducing amino acids (lysine, isoleucine and valine) [1,31].

The culture broth of each of the wild-type and mutant strains was harvested at three different growth stages [i.e. early exponential growth phase (EE), middle exponential growth phase (ME) and early stationary phase (ES)], and total intracellular proteins were extracted from disrupted cell pellets after centrifugation. For each protein sample, two-dimensional SDS/PAGE was repeated 4–8 times, and after silver staining an average 2-DE image was constructed for comparative image analysis using the software ImageMaster (Amersham Biosciences). On

Table 1 The 12 metabolic enzymes involved in the 101 proteins showing more than 30 % difference in intracellular protein level (i.e. spot intensity) between the mutant and wild-type strains

After comparative analyses of 2-DE images, 101 protein spots were selected, and proteins were identified by peptide mass fingerprinting after MALDI-TOF analysis. Accession number refers to the Swiss-PROT database. MM, molecular mass.

Spot no.	Gene name	Protein name	pI	MM (kDa)	Database accession no.	Mass matched (%)*
1	*ASPA*	Aspartate ammonia-lyase (aspartase)	5.2	52.36	P04422	58.8
2	*TDH*	Threonine dehydrogenase	5.9	37.24	P07913	76.9
3	*YJGB*	Hypothetical zinc-type alcohol dehydrogenase	5.9	36.50	P27250	57.1
4	*PFKB*	Phosphofuctokinase-2	5.7	32.39	P06999	66.7
5	*DAPA*	Dihydropicolinate synthetase	5.8	31.37	P05640	64.3
6	*METC*	Cystathionine β-lyase	6.0	43.21	P06721	78.9
7	*GLTA*	Citrate synthase	6.2	48.06	P00891	76.9
8	*PYKF*	Pyruvate kinase (PK-1)	5.8	50.73	P14178	62.5
9	*LEUC*	3-Isopropylmalate dehydratase large subunit (isopropylmalate isomerase)	5.9	49.91	P30127	69.2
10	*ADHC*	Alcohol dehydrogenase	5.9	39.36	P25437	70.6
11	*ACCA*	Acetyl-CoA carboxylase carboxyltransferase	5.8	35.24	P30867	58.8
12	*MDH*	Malate dehydrogenase	5.8	29.99	P06994	61.5

* Mass tolerance in protein identification through peptide mass fingerprinting was 10 p.p.m.

every average gel image, approx. 1000 spots were visualized and the 2-DE images for the wild-type and mutant strains were systematically compared at each growth stage (EE, ME or ES). Through this comparative image analysis, we noticed that 101 intracellular proteins showed more than 30 % difference in spot intensity between the wild-type and the mutant *E. coli*. MALDI–TOF analysis for each protein spot and subsequent peptide mass fingerprinting using Expasy database enabled identification of 12 metabolic enzymes out of the 101 proteins, as listed in Table 1, which are involved in glycolysis, tricarboxylic acid cycle and threonine biosynthesis (Figure 1). The time-course variation of the spot intensities of the 12 metabolic enzymes was estimated as presented in Figure 2 (panels 1–12). It is surprising to note that the difference in each enzyme level (spot intensity) between wild-type and mutant strain was more than 30-fold (Figure 2). It seems, therefore, reasonable to presume that the threonine oversynthesis resulted from altered conversion rate of key metabolic intermediates causing significant flux changes.

Estimation of threonine overproduction metabolism in the *E. coli* mutant

By comparative analysis between two *E. coli* proteomes, it was possible to observe the differences in metabolic enzyme synthesis related to threonine biosynthesis and understand how the metabolic flux has been changed in *E. coli* mutant. As presented below, we described modified metabolic pathways of threonine-overproducing *E. coli* mutant on the basis of the differences in synthesis level of metabolic enzymes catalysing threonine synthesis and degradation.

Metabolic pathway from glucose to aspartate

On comparison with the wild-type proteome, we noticed that synthesis levels of citrate synthase and malate dehydrogenase of the mutant were significantly different, i.e. a negligible synthesis of citrate synthase (Figure 2, panel 7) and more than 35-fold increase in malate dehydrogenase synthesis level (Figure 2, panel 12) in the mutant. As illustrated in Scheme 1(a), it is therefore reasonable to assume that a significant amount of oxaloacetate accumulates in the mutant and hence the overall metabolic flow seems to be directed towards the aspartate biosynthetic route. The unusual accumulation of oxaloacetate in the tricarboxylic acid cycle seems to cause the metabolic imbalance that may explain the repressed growth of the threonine-overproducing mutant. It has been reported that uncontrolled or deregulated metabolic pathways lead to metabolic imbalance and suboptimal productivity [32,33], and hence the alteration of metabolic enzyme synthesis could disturb the balanced metabolite flux and might exert a significant burden on an optimal cellular growth.

We also observed that the protein level of phosphofructokinase-2 (spot 4) catalysing the conversion of fructose 6-phosphate into fructose 1,6-bisphosphate was 380-fold higher in the mutant at the early stationary phase of growth (Figure 2, panel 4, and Scheme 1a). Similarly, another enzyme in the glycolysis pathway, pyruvate kinase (spot 8) was also oversynthesized in the mutant (Figure 2, panel 8, and Scheme 1a). The increased synthesis of glycolytic enzymes might result from the cellular effort to overcome the metabolic imbalance in tricarboxylic acid cycle, discussed above. That is, the mutant catabolism might be modulated towards increasing the supply of pyruvate and hence acetyl-CoA as a means to restore the reduced synthesis of citrate, although the repressed cell growth was inevitable during the cultivation. At the same time, other metabolic enzymes such as isopropylmalate isomerase (spot 9), alcohol dehydrogenase (spot 10), zinc-type alcohol dehydrogenase (spot 3), and acetyl-CoA carboxylase (spot 11) were oversynthesized to expedite probably the conversion of excessively accumulated pyruvate or acetyl-CoA, if any (Scheme 1a).

Metabolic pathway from aspartate to threonine

Threonine biosynthesis from aspartate was performed through five metabolic steps under the control of five key enzymes (i.e. aspartate kinase, aspartate semialdehyde dehydrogenase, homoserine dehydrogenase, homoserine kinase and threonine synthase) [34,35]. It is well known that the activity of aspartate kinase is regulated via negative feedback control by threonine and, moreover, homoserine dehydrogenase and homoserine kinase are partially repressed by accumulated threonine in *E. coli* pathway [15]. Based on this regulation mechanism, the more threonine-productive *E. coli* strains were developed by either introducing the feedback-resistant enzymes (i.e. aspartate kinase, homoserine dehydrogenase and homoserine kinase that are insensitive to

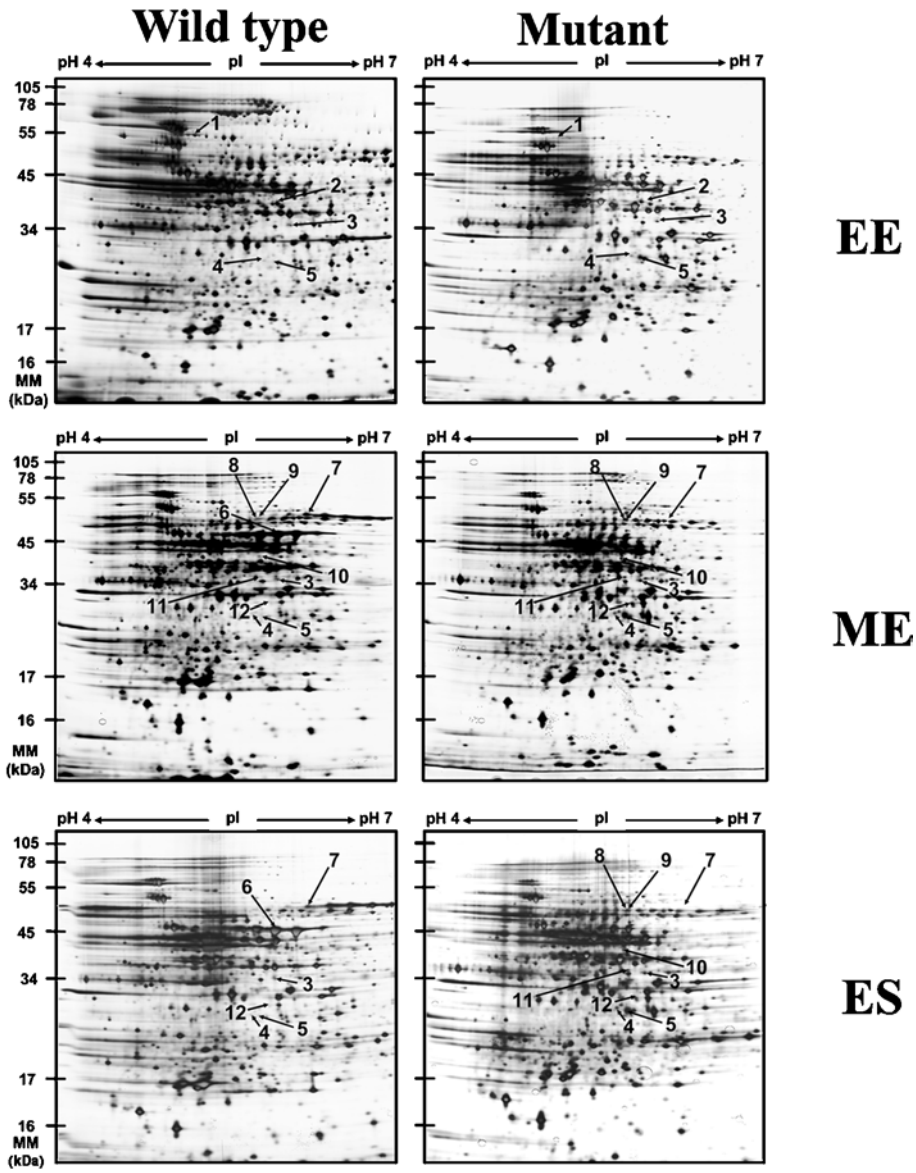

Figure 1 Silver-stained two-dimensional SDS/polyacrylamide gels showing 12 metabolic enzyme spots listed in Table 1

EE, early exponential growth phase; ME, middle exponential growth phase; ES, early stationary phase.

threonine inhibition) or gene expression amplification of the cognate key enzymes [2,15,18,35,36]. On the other hand, inhibition of the threonine degradation pathway may be another effective way of increasing threonine production level, although this approach has not been reported with detailed metabolic analysis. As discussed below, we observed the significant repression of metabolic degradation of threonine and its precursors, which seems to contribute significantly towards the threonine oversynthesis in the mutant strain.

Aspartate is converted into either fumarate or aspartyl β-phosphate, which is an intermediate precursor in the threonine synthetic route (Scheme 1b). Figure 2 (panel 1) shows that the synthesis of aspartase (aspartate ammonia-lyase, ASPA) was significantly inhibited in the mutant strain. Accumulated aspartate might be metabolized towards synthesizing threonine without unfavourable degradation to fumarate and ammonia (Scheme 1b). Even in the wild-type strain, the synthesis of ASPA was noticed only in the early exponential growth phase (EE) (Figure 2, panel 1). The reason is not clear, but it can be presumed that degradation of aspartate rarely occurs during the post-EE period, when there must be increased cellular need for the major amino acids (as the aspartate family) to support active cell growth and cellular maintenance. This finding that ASPA synthesis occurs only in the EE period is somewhat coincident with the previous report that under initial non-steady-state conditions, the pathway flux of aspartate consumption exhibits greater sensitivity to the aspartate concentration compared with the threonine concentration [15,18].

The time-course profile of TDH (threonine dehydrogenase) synthesis that is responsible for the degradation of threonine is quite similar to the case of ASPA in both the wild-type and mutant strains (Figure 2, panel 2). For the wild-type strain, augmented cellular requirements for threonine after the EE period seemed to induce the repression of TDH synthesis (Scheme 1b). The TDH synthesis was repressed all the time during the whole period of the mutant growth (Figure 2, panel 2), which must be a more

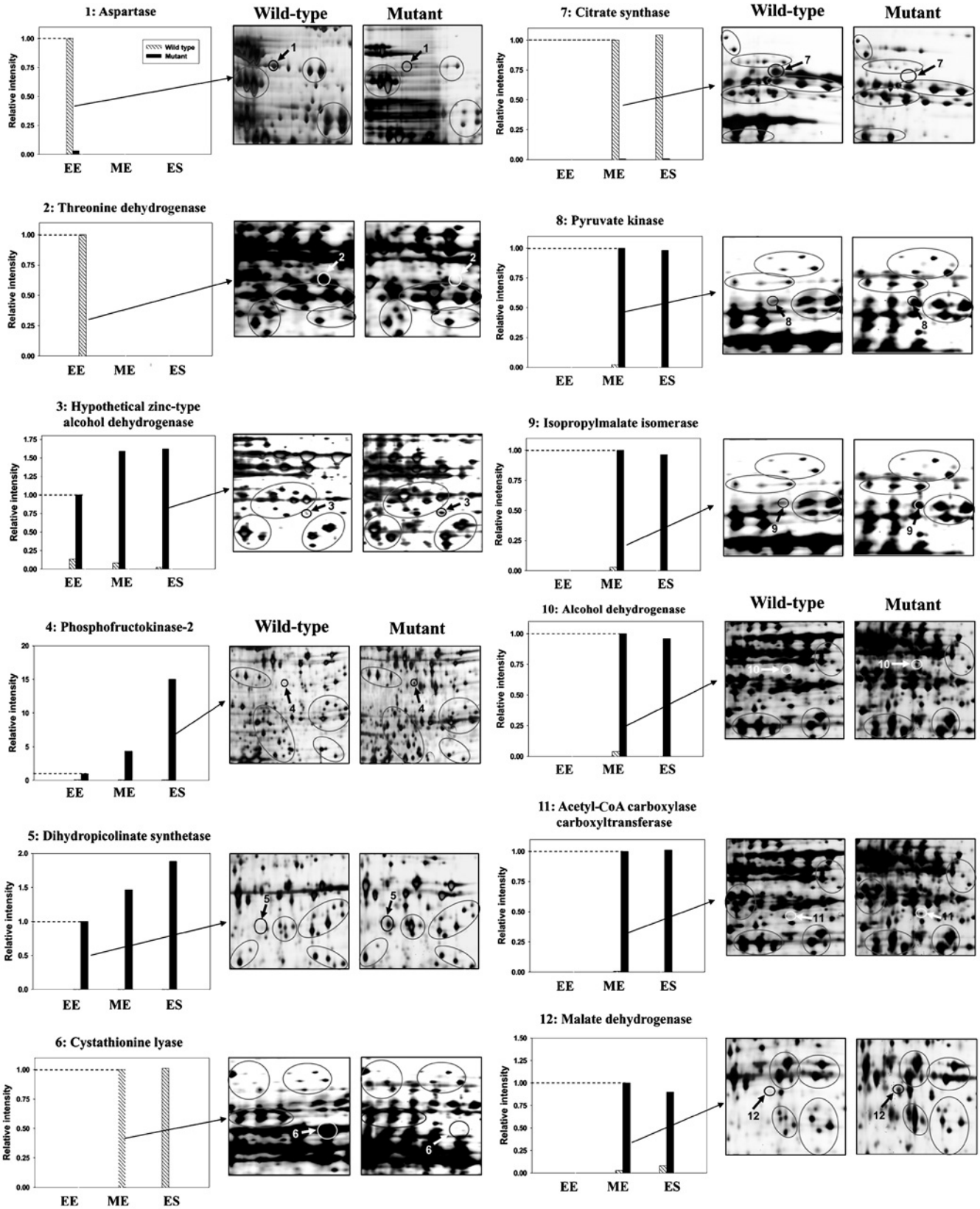

Figure 2 Time-course variations in spot intensity of 12 metabolic enzymes (1–12) in both mutant and wild-type

Black and striped columns indicate spot intensity from mutant and wild-type respectively. The encircled gel spots are the constantly visualized spots both in wild-type and mutant.

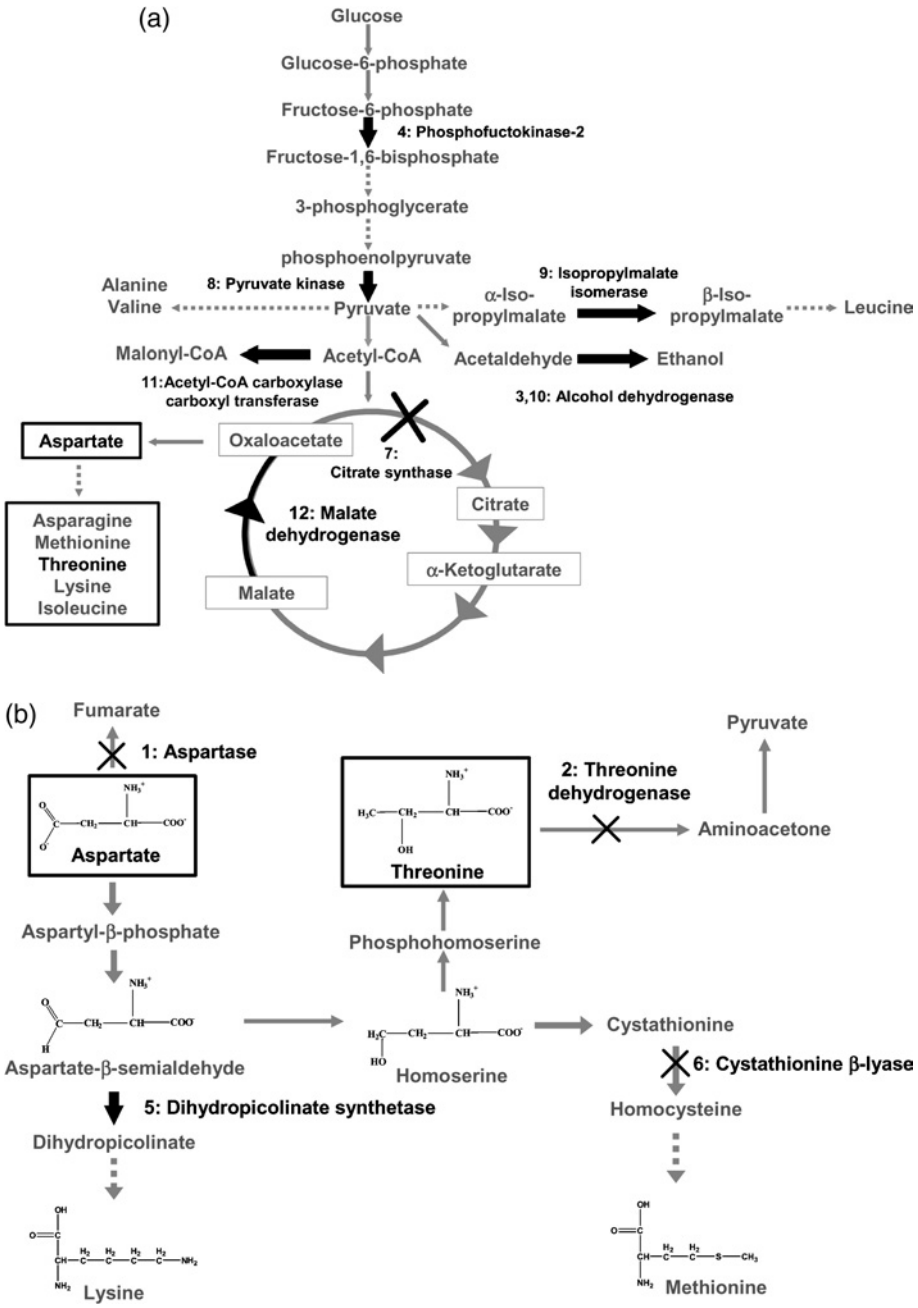

Scheme 1 Proposed overview of altered metabolic pathways of mutant, showing conversion of (a) glucose into aspartate and (b) aspartate into threonine

Thick arrow represents that the metabolic conversion was significantly activated. Probably this is due to increased protein level (i.e. spot intensity) of the corresponding metabolic enzyme. Also, cross mark indicates that the metabolic conversion was severely repressed. The cause for this may be a far lowered protein level of the corresponding metabolic enzyme.

favourable condition for the threonine overproduction without breakdown to aminoacetone.

The altered enzyme synthesis for threonine overproduction can also be elucidated with Figure 2 (panel 6) and Scheme 1(b). As presented in Scheme 1(b), METC (cystathionine β-lyase) catalyses the conversion of cystathionine into homocysteine that is finally converted into methionine. In the wild-type *E. coli*, the synthesis of METC was highly promoted in the middle exponential growth and early stationary phase (Figure 2, panel 6). In the mutant strain, however, the METC synthesis was almost completely prohibited during the whole period of growth (Figure 2, panel 6). As illustrated in Scheme 1(b), the inhibition of METC synthesis seems to increase significantly the intracellular amount of homoserine that is a key intermediate for the threonine biosynthesis. Since any noticeable amount of lysine was never detected in the culture broth (results not shown), the enhanced level of dihydropicolinate synthetase in the mutant does not seem to contribute towards increasing the level of metabolic intermediates involved in the lysine synthetic pathway.

Conclusions

2-DE was very useful in understanding the quantitative proteomic responses of threonine-overproducing mutant by analysing in

detail the time-course variations in the protein level. Comparative analyses of the wild-type and mutant proteomes showed that threonine overproduction accompanied the significant changes in the synthesis level of key metabolic enzymes involved in threonine biosynthesis and degradation pathway. As a result, it is strongly suggested that the altered metabolic conversion leading to the accumulation of oxaloacetate and aspartate and the inhibition of degradation pathways of threonine and precursors played a critical role in producing a large amount of threonine from the mutant. More complete information about the overall regulation characteristics of threonine overproduction would be achieved through a detailed analysis of transcriptomic responses at the gene expression level.

REFERENCES

1 Eggeling, L., Morbach, S. and Sahm, H. (1997) The fruits of molecular physiology: engineering the L-isoleusine biosynthesis pathway in *Corynebacterium glutamicum*. J. Biotechnol. **56**, 167–182
2 Debabov, V. G. (2003) The threonine story. Adv. Biochem. Eng. Biotechnol. **79**, 113–136
3 Pfefferle, W., Mockel, B., Bathe, B. and Marx, A. (2003) Biotechnological manufacture of lysine. Adv. Biochem. Eng. Biotechnol. **79**, 59–112
4 Ikeda, M. and Katsumata, R. (1994) Transport of aromatic amino acids and its influence on overproduction of the amino acids in *Corynebacterium glutamicum*. J. Ferment. Bioeng. **78**, 420–425
5 Farfan, M. J. and Calderon, I. L. (2000) Enrichment of threonine content in *Saccharomyces cerevisiae* by pathway engineering. Enzyme Microbiol. Technol. **26**, 763–770
6 Kazuyuki, O., Kuniki, K. and Masato, I. (1997) Hyperproduction of L-threonine by an *Escherichia coli* mutant with impaired L-threonine uptake. Biosci. Biotechnol. Biochem. **61**, 1887–1892
7 Ishida, M., Sato, K., Hashiguchi, K. I., Ito, H., Enei, H. and Nakamori, S. (1993) High fermentative production of L-threonine from acetate by a *Brevibacterium flavum* stabilized strain transformed with a recombinant plasmid carrying the *Escherichia coli* the operon. Biosci. Biotechnol. Biochem. **57**, 1755–1756
8 Ishida, M., Kawashima, H., Sato, K., Hashiguchi, K. I., Ito, H., Enei, H. and Nakamori, S. (1994) Factors improving L-threonine production by a three L-threonine biosynthetic genes-amplified recombinant strain of *Brevibacterium lactofermentum*. Biosci. Biotechnol. Biochem. **58**, 768–770
9 Rais, B., Chassagnole, C. and Mazat, J. P. (1995) Control of threonine pathway in *E. coli*. Application to biotechnologies. Acta Biotheor. **43**, 285–297
10 Reinscheid, D. J., Kronemeyer, W., Eggeling, L., Eikmanns, B. J. and Sahm, H. (1994) Stable expression of hom-1-theB in *Corynebacterium glutamicum* and its effect on the carbon flux to threonine and related amino acids. Appl. Environ. Microbiol. **60**, 126–132
11 Shiio, I., Sugimoto, S. I., Yoshino, H. and Kawamura, K. (1990) Isolation and properties of threonine-producing mutants with both dihydrodipicolinate synthase defect and feedback-resistant homoserine dehydrogenase from *Brevibacterium flavum*. Agric. Biol. Chem. **54**, 1505–1511
12 Colon, G. E., Jetten, M. S., Nguyen, T. T., Gubler, M. E., Follettie, M. T., Sinskey, A. J. and Stephanopoulos, G. (1995) Effect of inducible theB expression on amino acid production in *Corynebacterium lactofermentum* ATCC 21799. Appl. Environ. Microbiol. **61**, 74–78
13 Templeton, B. A. and Savageau, M. A. (1974) Transport of biosynthetic intermediates: homoserine and threonine uptake in *Escherichia coli*. J. Bacteriol. **117**, 1002–1009
14 Hama, H., Shimamoto, T., Tsuda, M. and Tsuchiya, T. (1987) Properties of a Na^+-coupled serine–threonine transport system in *Escherichia coli*. Biochim. Biophys. Acta **905**, 231–239
15 Chassagnole, C., Fell, D. A., Rais, B., Kudla, B. and Mazat, J. P. (2001) Control of the threonine-synthesis pathway in *Escherichia coli*: a theoretical and experimental approach. Biochem. J. **356**, 433–444
16 Sumantran, N. V., Schweizer, H. P. and Datta, P. (1990) Novel membrane-associated threonine permease encoded by the tdcC gene of *Escherichia coli*. J. Bacteriol. **172**, 4288–4294
17 Chassagnole, C., Rais, B., Quentin, E., Fell, D. A. and Mazat, J. P. (2001) An integrated study of threonine-pathway enzyme kinetics in *Escherichia coli*. Biochem. J. **356**, 415–423
18 Rais, B., Chassagnole, C., Letellier, T., Fell, D. A. and Mazat, J. P. (2001) Threonine synthesis from aspartate in *Escherichia coli* cell-free extracts: pathway dynamics. Biochem. J. **356**, 425–432
19 Shames, S. L., Ash, D. E., Wedler, F. C. and Villafranca, J. J. (1984) Interaction of aspartate and aspartate-derived antimetabolites with the enzymes of the threonine biosynthetic pathway of *Escherichia coli*. J. Biol. Chem. **259**, 15331–15339
20 Alban, A., David, S. O., Bjorkesten, L., Andersson, C., Sloge, E., Lewis, S. and Currie, I. (2003) A novel experimental design for comparative two-dimensional gel analysis: two-dimensional difference gel electrophoresis incorporating a pooled internal standard. Proteomics **3**, 36–44
21 Gorg, A., Obermaier, C., Boguth, G., Harder, A., Scheibe, B., Wildgruber, R. and Weiss, W. (2000) The current state of two-dimensional electrophoresis with immobilized pH gradients. Electrophoresis **21**, 1037–1053
22 Williams, K. L. (1999) Genomes and proteomes: towards a multidimensional view of biology. Electrophoresis **20**, 678–688
23 Kirkpatrick, C., Maurer, L. M., Oyelakin, N. E., Yoncheva, Y. N., Maurer, R. and Slonczewski, J. L. (2001) Acetate and formate stress: opposite responses in the proteome of *Escherichia coli*. J. Bacteriol. **183**, 6466–6477
24 Champion, K. M., Nishihara, J. C., Joly, J. C. and Arnott, D. (2001) Similarity of the *Escherichia coli* proteome upon completion of different biopharmaceutical fermentation processes. Proteomics **1**, 1133–1148
25 Han, M. J., Yoon, S. S. and Lee, S. Y. (2001) Proteomics analysis of metabolically engineered *Escherichia coli* producing poly(3-hydroxybutyrate). J. Bacteriol. **183**, 301–308
26 Tonella, L., Hoogland, C., Binz, P. A., Appel, R. D., Hochstrasser, D. F. and Sanchez, J. C. (2001) New perspectives in the *Escherichia coli* proteome investigation. Proteomics **1**, 409–423
27 Lee, J. H., Lee, D. E., Lee, B. U. and Kim, H. S. (2003) Global analyses of transcriptome and proteome of a parent strain and an L-threonine-overproducing mutant strain. J. Bacteriol. **185**, 5442–5451
28 Theze, J. and Saint-Girons, I. (1974) The threonine locus of *Escherichia coli* K-12: genetic structure and evidence for an operon. J. Bacteriol. **42**, 59–73
29 Rabilloud, T. (1999) Silver staining of 2-D electrophoresis gels. Methods Mol. Biol. **112**, 297–305
30 Gharahdaghi, F., Weinberg, C. R., Meagher, D. A., Imai, B. S. and Mische, S. M. (1999) Mass spectrometric identification of proteins from silver-stained polyacrylamide gel: a method for the removal of silver ions to enhance sensitivity. Electrophoresis **20**, 601–605
31 Kisumi, M., Komatsubara, S. and Chibata, I. (1977) Enhancement of isoleucine hydroxamate-mediated growth inhibition and improvement of isoleucine-producing strains of *Serratia marcescens*. Appl. Environ. Microbiol. **34**, 647–653
32 Farmer, R. F. and Liao, J. C. (2000) Improving lycopene production in *Escherichia coli* by engineering metabolic control. Nat. Biotechnol. **18**, 533–537
33 Kurland, C. G. and Dong, H. (1996) Bacterial growth inhibition by overproduction of protein. Mol. Microbiol. **21**, 1–4
34 Szczesiul, M. and Wampler, D. E. (1976) Regulation of a metabolic system *in vitro*: synthesis of threonine from aspartic acid. Biochemistry **15**, 2236–2244
35 Patte, J. C., Truffa-Bachi, P. and Cohen, G. N. (1966) The threonine sensitive homoserine dehydrogenase and aspartokinase activities of *Escherichia coli*. Biochim. Biophys. Acta **128**, 426–439
36 Shiio, I., Nakamori, S. and Sano, K. (1971) Fermentation production of L-threonine. U.S. patent 3580810

Received 18 November 2003/21 April 2004; accepted 23 April 2004
Published as BJ Immediate Publication 23 April 2004, DOI 10.1042/BJ20031763